JACS
JOURNAL OF THE AMERICAN CHEMICAL SOCIETY

ARTICLE

pubs.acs.org/JACS

Physical−Chemical Aspects of Protein Corona: Relevance to *in Vitro* and *in Vivo* Biological Impacts of Nanoparticles

Marco P. Monopoli,[†,‡] Dorota Walczyk,[†] Abigail Campbell,[†] Giuliano Elia,[‡] Iseult Lynch,[†] Francesca Baldelli Bombelli,[*,†] and Kenneth A. Dawson[*,†]

[†]Centre for BioNano Interactions, School of Chemistry and Chemical Biology and UCD Conway Institute for Biomolecular and Biomedical Research, University College Dublin, Belfield, Dublin 4, Ireland

[‡]Mass Spectrometry Resource, UCD Conway Institute for Biomolecular and Biomedical Research, University College Dublin, Belfield, Dublin 4, Ireland

Supporting Information

ABSTRACT:

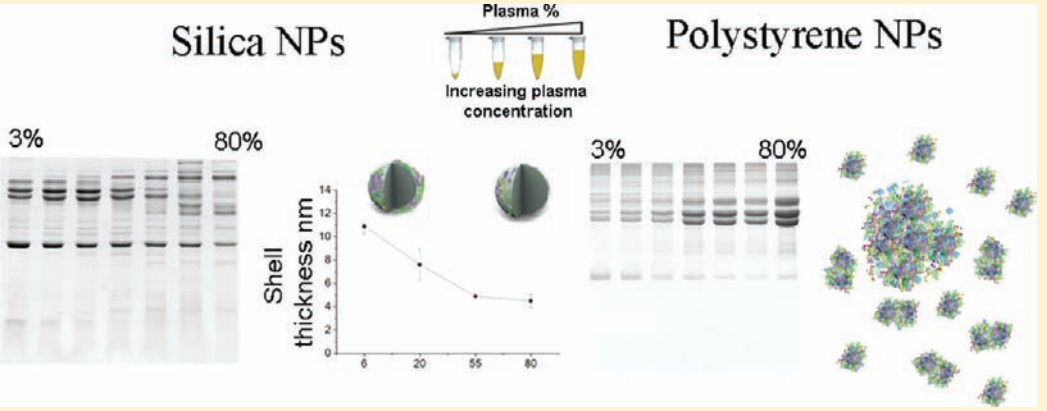

It is now clearly emerging that besides size and shape, the other primary defining element of nanoscale objects in biological media is their long-lived protein ("hard") corona. This corona may be expressed as a durable, stabilizing coating of the bare surface of nanoparticle (NP) monomers, or it may be reflected in different subpopulations of particle assemblies, each presenting a durable protein coating. Using the approach and concepts of physical chemistry, we relate studies on the composition of the protein corona at different plasma concentrations with structural data on the complexes both *in situ* and free from excess plasma. This enables a high degree of confidence in the meaning of the hard protein corona in a biological context. Here, we present the protein adsorption for two compositionally different NPs, namely sulfonated polystyrene and silica NPs. NP−protein complexes are characterized by differential centrifugal sedimentation, dynamic light scattering, and zeta-potential both *in situ* and once isolated from plasma as a function of the protein/NP surface area ratio. We then introduce a semiquantitative determination of their hard corona composition using one-dimensional sodium dodecyl sulfate−polyacrylamide gel electrophoresis and electrospray liquid chromatography mass spectrometry, which allows us to follow the total binding isotherms for the particles, identifying simultaneously the nature and amount of the most relevant proteins as a function of the plasma concentration. We find that the hard corona can evolve quite significantly as one passes from protein concentrations appropriate to *in vitro* cell studies to those present in *in vivo* studies, which has deep implications for *in vitro*−*in vivo* extrapolations and will require some consideration in the future.

INTRODUCTION

It is increasingly accepted that the "surfaces" of nanoparticles (NPs) in a biological environment are modified by the adsorption of biomolecules such as proteins and lipids, leading to a biomolecular interface organization that may be loosely divided into two components named the "hard" and "soft" coronas with (respectively) "long" and "short" typical exchange times.[1−5] Indeed, the lifetime of the hard corona for a number of typical materials has been shown to be many hours,[4] sufficiently long that, for many cellular and higher level biological and physiological contexts, this corona defines the biological identity of the particle. It is increasingly accepted that the overall scale of even nonspecific cell−particle interactions is determined by the degree of "screening" of the NP surface by the corona,[6] and examples of novel biological processes due to expression of functional epitopes on the corona are emerging.[7]

Received: August 22, 2010
Published: February 2, 2011

ACS Publications © 2011 American Chemical Society

dx.doi.org/10.1021/ja107583h | *J. Am. Chem. Soc.* 2011, 133, 2525–2534

In a typical biological environment, many biomolecules (for example, blood plasma contains several thousand different proteins whose abundance varies by 12 orders of magnitude) compete for the limited NP surface, leading to a combinatorial offering of molecules to that surface. Here we will focus on the role of proteins, but it should be emphasized that many other molecules are present in the corona, including a range of different lipids.[8]

Over time, the most abundant protein (it having bound first) is displaced by those with higher affinity, and the resulting biomolecule "hard corona" contains only a few proteins in a relatively immobile layer, with a more loosely bound layer that is less well-understood.[1,2] Here we emphasize that the composition of the corona itself may depend on the ratio of available NP surface to protein for different materials. Indeed, such effects may be so striking that the biological identity of the NP may change dramatically as the amount of protein in the environment changes. In particular, particles studied *in vitro* (at low serum dilutions) may bear little relation to those that exist *in vivo* (high protein concentration as, for example, in the blood), suggesting the need for a re-evaluation of how such studies should be planned in the future and how *in vitro*−*in vivo* extrapolations can be made.

There are many factors influencing the detailed nature of the NP biomolecule corona, with NP size, shape, surface charge, and solubility all playing a role in the interaction of the NPs with proteins. Nanoscale surface curvature strongly affects protein adsorption, so that protein-binding affinities for NPs surface are different than for their analogue bulk material[9,10] and the coronas associated with NPs of the same material but of different size can vary in composition.[11] In the sorts of biological fluids of interest here, there is considerable choice as to which molecules are finally selected to form the hard corona and in terms of their orientation at the surface and potentially their degree of unfolding, which allows the different interactions (charge, hydrophobic, etc.) to be progressively reduced as the layer is built up.[2,12−14] A general understanding of the impact of NP−protein interactions on the biological response to NPs *in vitro* and *in vivo* is, as yet, lacking.[15−17,14] Still, growing *in vivo* and *in vitro* evidence suggests that the interaction between NPs and plasma proteins and other blood components is a determining factor for the fate and impact of the particles. Certainly the adsorbed protein layer influences cellular uptake and may affect trafficking,[15,16] while *in vivo*, specific binding of proteins may affect particle biodistribution.[17−19] For example, adsorption of opsonins like fibrinogen, IgG, complement factor, etc. is believed to promote phagocytosis with removal of the NPs from the bloodstream,[20,21] while binding of dysopsonins like human serum albumin (HSA), apolipoproteins, etc. promotes prolonged circulation time in blood.[22] It may also be that apolipoprotein enrichment on NP surfaces promotes interaction with low-density lipoprotein receptors, resulting in transport across the blood−brain barrier.[23,24]

Here, we have studied plasma protein adsorption for two compositionally different NPs. "Hydrophobic" sulfonated polystyrene ($PSOSO_3$) NPs and hydrophilic silica (SiO_2) NPs are used to illustrate how a binding mechanism dominated by interactions composed of different contributions from hydrophobic, electrostatic, and H-bonding affects the resultant NP−protein corona structure and composition. NP−protein complexes have been characterized by differential centrifugal sedimentation (DCS), dynamic light scattering (DLS), and zeta-potential both *in situ* and once isolated from plasma (so-called "free from excess plasma" samples) as a function of the protein/NP surface area ratio. We then introduce a semiquantitative determination of their hard corona composition, using one-dimensional sodium dodecyl sulfate−polyacrylamide gel electrophoresis (1D PAGE) and electrospray liquid chromatography mass spectrometry (LC MS/MS). This allows us to follow the total binding isotherms for the particles, identifying simultaneously the nature and amount of the most relevant proteins as a function of the plasma concentration. This is the analogy to a multicomponent Langmuir adsorption isotherm, in which one allows for the full manifestation of competitive binding from thousands of different components. This allows us to illustrate more quantitatively the degree to which the biomolecule corona can change, depending on the biological environment.

RESULTS AND DISCUSSION

Structure of NP−Corona Complexes: Effect of Protein/NP Surface Area Ratio. Relatively monodisperse NPs, composed of $PSOSO_3$ or SiO_2 (200 and 50 nm, whose physical−chemical characterization is reported in Table S1 and Figure S1 in the Supporting Information), were exposed to increasing plasma concentrations for varying (fixed) time periods. The ratio between the total NP surface area available and the protein concentration was also fixed for the two NPs to enable us to relate the features of the resulting NP−protein complexes to the different protein−NP interactions involved in the two cases. Typical results after the hard corona has stabilized, spanning biologically relevant plasma concentrations, are reported.

Nanoparticles (200 nm $PSOSO_3$ and SiO_2) were incubated in human plasma for 1 h, and the resulting NP−protein complexes were separated from excess plasma by centrifugation and extensive washing to remove the unbound proteins (see "Sample Preparation" in the Materials section in the Supporting Information). Bound proteins — the hard corona — were first removed from the particles and then separated by 1D PAGE as explained in the Supporting Information.

Figure 1a,b illustrates SDS−PAGE results in which 200 nm SiO_2 and $PSOSO_3$ NPs were incubated in plasma concentrations from 3% to 80%, illustrating a clear difference in the protein corona composition and evolution trend for the two materials. With increasing plasma concentration, the intensity of typical bands in the $PSOSO_3$ NPs corona strongly increases (i.e., more proteins of the same type bind at higher concentrations). The most striking observation is that for SiO_2 NPs, the identity of the primary protein bands actually changes with increasing plasma concentration. A semiquantitative densitometry analysis of the bands, used to quantify the total amount of proteins in the corona at the different plasma concentrations (Figure 1c,d), shows that for $PSOSO_3$ NPs, the total amount of proteins clearly increases with increasing percentage of plasma, while for SiO_2 NPs, total bound protein decreases slightly with increasing plasma concentration. It is sometimes considered that higher levels of protein adsorption occur on hydrophobic flat surfaces than on hydrophilic ones.[25] This analysis has been done on the SDS−PAGE gel reported in Figure S2 in the Supporting Information, where we determined the protein corona of three samples (3%, 20%, and 80% plasma) measured in three independent replicates (biological replicates). The protein pattern for SiO_2 NPs changes significantly with increasing plasma concentration, suggesting that less plentiful competitive binding proteins, whose adhesion increases at higher percentages of human plasma, act as competitive binders and facilitate the desorption of proteins with lower binding affinity (Figure 1b).

DCS studies of the particle−protein complexes across the range of plasma concentrations of interest are revealing. Full

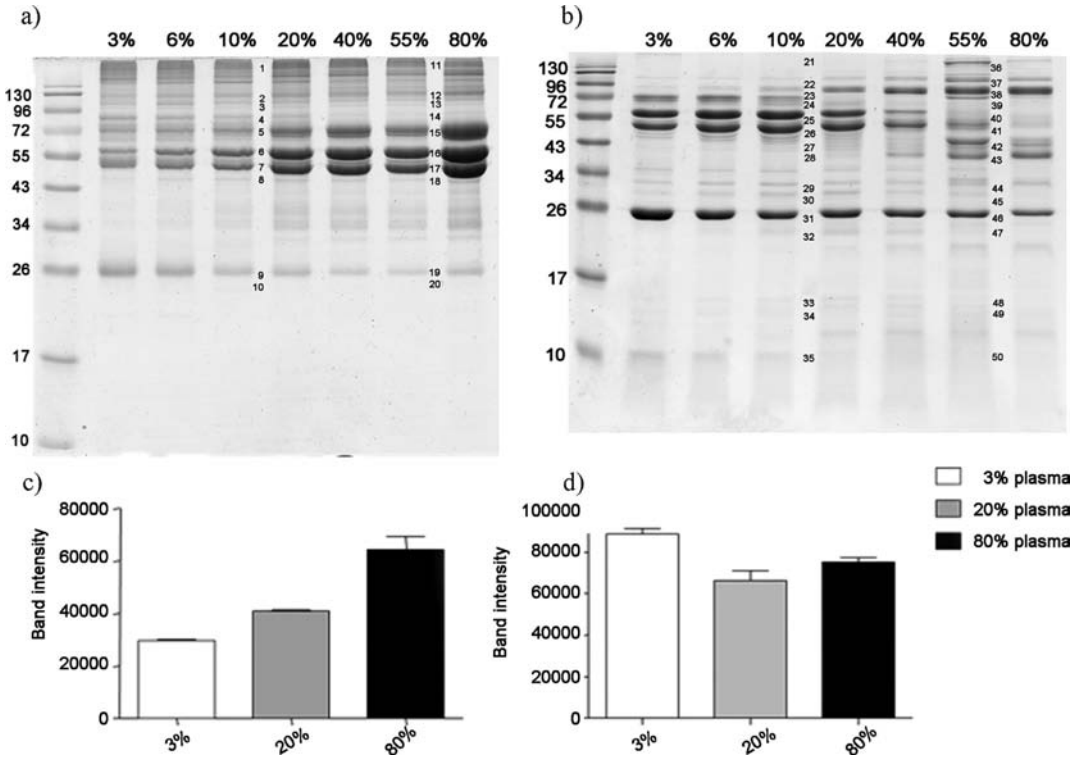

Figure 1. SDS−PAGE gel of human plasma proteins obtained from (a) 200 nm $PSOSO_3$ NP−protein complexes (b) 200 nm SiO_2 NP−protein complexes free from excess plasma following incubation at different plasma concentrations. The procedure to separate the proteins from the NPs is described in ref 3. The molecular weights of the proteins in the standard ladder are reported on the left for reference. The numbers reported close to the gel bands for 10% and 55% plasma indicate those bands that were cut out and analyzed with mass spectrometry. Histograms representing the total band intensity of proteins recovered from (c) 200 nm $PSOSO_3$ NPs and (d) 200 nm SiO_2 NPs incubated with 3%, 20% and 80% plasma concentration (see Figure S2 in the Supporting Information).

details of the DCS approach are given in the Methods section in the Supporting Information, but we note here that it can be made remarkably reproducible, with striking precision.[26] However, to identify the true size of an aggregate from DCS data, its shape and internal density distribution are required. Therefore, for monomeric NP−protein complexes, we compute the "true" size of the NP−protein complex and the corona size (thickness) using a simple core−shell two-density model involving the particle material and adsorbed protein/biomolecule densities. Details are given in the Methods sections in the Supporting Information.

The SiO_2 NP−corona samples used to prepare the gel reported in Figure 1b are studied both *in situ* in the presence of the excess plasma and as the isolated "hard corona" after spinning down, separation, and washing (Figure 2a,c). The particle size distributions of SiO_2 NP−protein hard corona complexes are relatively monodisperse and characterized by a broad distribution slightly shifted with respect to that of the bare NPs. One should note that SiO_2 NP−corona shifts must be corrected using the core−shell model (see Methods section in the Supporting Information) to obtain the protein shell thickness. Corona thicknesses are presented in Figure 2b as a function of the plasma concentration; interestingly, they become smaller at higher plasma concentrations. DCS experiments on the same samples were also performed *in situ* (in the biological fluid after 1 h of incubation), and the results, reported in Figure 2c,d, follow the same general trend as for the isolated protein−NP complexes. Uncertainties in hard corona sizes, studied in phosphate-buffered saline (PBS), and those determined *in situ* include experimental complications due to microlubrication effects (not yet understood at the quantitative level) from the residual protein for *in situ* studies, as well as the fitted hard corona protein density for both samples.[4] However, the raw data themselves are highly reproducible. We have also provided a theoretical calculation to determine the amount of total protein necessary to form a shell such as that obtained from DCS at the different plasma concentrations in Figure S3 in the Supporting Information. The total protein content is in large excess, even for the lowest plasma concentration used in the corona experiments.

In DLS, the size distribution of SiO_2 NP−protein complexes is shifted with respect to that of the bare NPs. Initial formation (at low plasma concentration) of the hard corona leads, as expected, to a significantly larger hydrodynamic diameter, followed by a sharp decrease and then little variation with increasing plasma concentration (Table 1). Zeta-potential values for SiO_2 NP−protein complexes indicate that the relatively high ζ-potential in PBS (−25 mV) is reduced (to approximately −11 mV) even at low plasma concentrations, suggesting that the protein coating itself is the main source of the particle stability in plasma. Both DLS and ζ-potential measurements suggest that even for low plasma concentrations, a protein layer is formed on the particles, even if it then evolves somewhat with increasing plasma concentration. Typical TEM images for 200 nm SiO_2 NPs before and after incubation in plasma are reported in Figure S4 in the Supporting Information.

Evidently DCS, which yields a more direct estimation of the corona size than the hydrodynamic size from DLS, gives evidence of much more nuanced evolutions of the corona layer with increasing concentration, and this seems quite consistent with the proteomics studies. DCS results for $PSOSO_3$ NPs suggest much more particle aggregation (Figure S5 in the Supporting

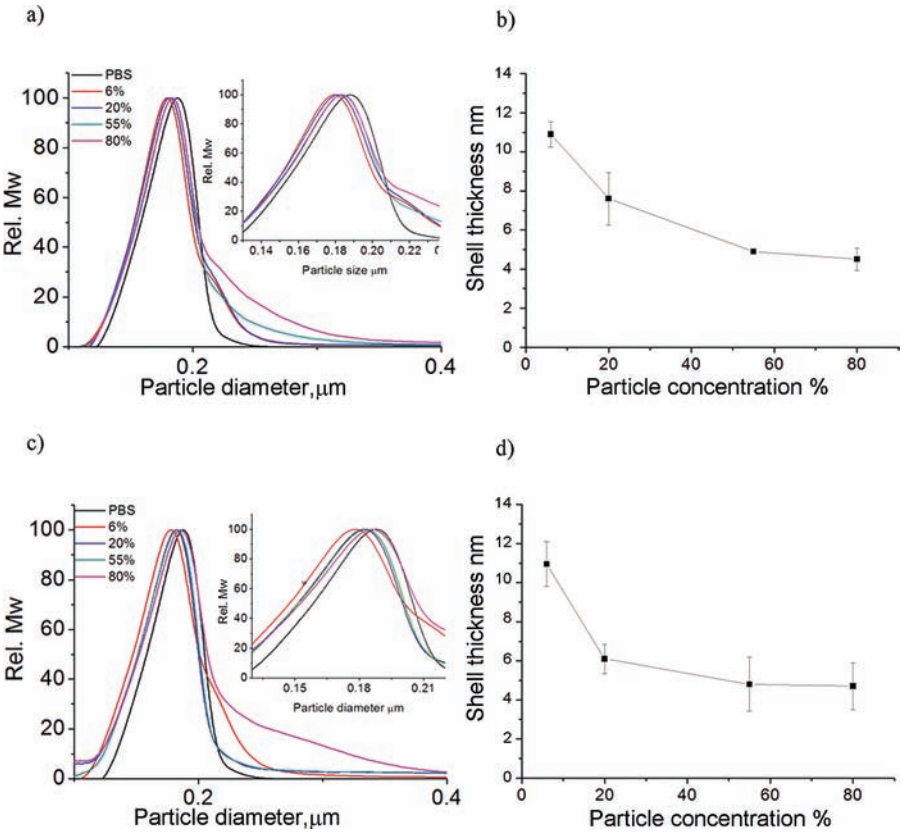

Figure 2. (a) DCS experiments of 200 nm SiO_2 particle−corona complexes free from excess plasma and diluted in PBS. The particle−corona complexes were isolated after 1 h of incubation in plasma solution at different concentrations, as shown in the legend. (b) Shell thickness of 200 nm SiO_2 NP−plasma complexes free from excess plasma calculated using a core−shell model (see Supporting Information) and expressed as a function of increasing plasma concentration. (c) DCS experiments of 200 nm SiO_2 particle−corona complexes *in situ* after incubation in plasma solutions at different concentrations. (d) Shell thickness of 200 nm SiO_2 NP−plasma complexes *in situ* after incubation in plasma solutions at different concentrations.

Table 1. DLS and Zeta-Potential Data of 200 nm SiO_2 Particle−Corona Complexes Free from Excess Plasma, Obtained Following Incubation at Different Plasma Concentrations[a]

% plasma	D_H[b] (nm)	PDI[c]	$\langle D_H \rangle$[d] (nm)	ζ-potential (mV)
0	205.0 ± 0.8	0.04	215.0 ± 0.8	−25.2 ± 0.2
3	266.6 ± 1.7	0.12	292.1 ± 1.7	−12.1 ± 2.1
6	238.0 ± 3.1	0.09	257.4 ± 3.1	−8.4 ± 0.7
20	235.1 ± 0.9	0.09	259.7 ± 0.9	−10.4 ± 0.6
55	245.8 ± 3.5	0.13	269.5 ± 3.5	−11.1 ± 1.0
80	238.1 ± 0.5	0.07	257.7 ± 0.5	−10.2 ± 0.3

[a] The error bars are expressed as the standard deviation of five measurements, with each measurement being an average of six repetitions of 1 min. [b] *z*-average hydrodynamic diameter extracted by cumulant analysis of the data. [c] Polydispersity index from cumulant fitting. [d] Average hydrodynamic diameter determined from CONTIN size distribution.

Information), and fewer simple conclusions can be drawn. Particle monomers, rotationally averaged dimers, and trimers with shifted peaks (thereby allowing a determination of the size of the corona layer) are present, as are particle aggregates (nominally around 0.7 μm). Supplementary DLS sizes confirm the DCS conclusion that $PSOSO_3$ NPs undergo extensive aggregation at all plasma concentrations (data not shown). These aggregates are quite intriguing, for (though they are absent for bare particles in PBS) similar peaks are present in the DCS data of pure plasma under the same experimental conditions (see Figure S6 in the Supporting Information). Since polystyrene and proteins have relatively similar densities, we can interpret the data (even in the absence of structural information) to mean that polystyrene NPs embed themselves within these plasma protein clusters, leading to the shifted particle peaks observed in the presence of plasma (see Figure S5). Comparisons with studies carried out *in situ* indicate that the protein−NP complexes are comparable to the isolated complexes, at least for sizes less than 0.4 μm, where centrifugal forces may be more limited. Despite the complexity of the sample, particle diameters with protein coronas can still be isolated from the monomer peaks and their evolution with increasing plasma determined. Again, the thickness of the protein shell for particle monomer−protein complexes may be calculated by assuming a core−shell model as reported in Table 2. As with many other systems, the addition of more protein (more concentrated plasma) tends to lead to a thicker protein corona, highlighting the distinctiveness of the SiO_2 NPs. It is surprising that, despite the complexity of the $PSOSO_3$ NPs system, results for populations of multimers, aggregates, and the proteins extracted from their surfaces are highly reproducible. However, for such complex mixtures of protein-coated assemblies, whatever the local curvature issues, there is no guarantee that each of these clusters has an identical protein corona composition. It is most important to stress that the biological implications of these observations are even subtler, as there is also a biological size effect such that clearance cells recognize objects somewhat larger than (roughly) 300 nm easily,

dx.doi.org/10.1021/ja107583h |*J. Am. Chem. Soc.* 2011, 133, 2525–2534

Table 2. Size of the Protein Shell of 200 nm $PSOSO_3$ Monomer Particle−Protein Complexes Free from Excess Plasma and *in Situ*, Extracted from the DCS Experiments Shown in Figure S5 in the Supporting Information

	hard corona		*in situ*	
% plasma	D^a (nm)	δ^b (nm)	D^a (nm)	δ^b (nm)
0	262.0 ± 0.1		262 ± 5.24	
5	300.2 ± 0.3	4.9 ± 0.3	304.7 ± 0.1	5.4 ± 0.1
20	313.3 ± 0.2	6.6 ± 0.2	328.0 ± 0.2	8.7 ± 0.2
80	332.5 ± 0.2	9.6 ± 0.2	362.6 ± 0.3	14.0 ± 0.3

[a] Error bars are estimated as the standard deviation of three repetitions. [b] Estimated protein shell size associated with monomeric NP−protein complexes of 200 nm $PSOSO_3$ by analyzing the DCS data in Figure S5, as explained in the Methods section in the Supporting Information.

depending on their protein coating. Given the observations here for $PSOSO_3$ NPs, one can envisage a multiplicity of objects, with different protein coatings, eliciting a variety of biological effects in different cell types. There are many signs in the nanobiology, nanomedicine, and nanosafety literature that such complexities are leading to (apparent) irreproducibility and to some degree of confusion. The desire to highlight this issue led us to choose $PSOSO_3$ NPs as an interesting example for detailed study.

Determination of the Protein Corona Composition. A more detailed study of the surface adsorption, from which we expect to be able to rationalize phenomena associated with the SiO_2 NP hard corona in some detail, has been performed. Thus, Figure 1a,b shows *de facto* the equivalent of the Langmuir adsorption isotherm for a multicomponent fluid. In Figure 3a,b, we show the relative densitometry results (the intensity of each band is divided by the total intensity of the lane) of relevant bands from the gels in Figure 1a,b as a function of the plasma concentration during incubation. Within the limits of gel separation methodologies, this provides a semiquantitative description of the variations in the band intensities that are clearly visible in Figure 1.

The bands of interest, labeled as in Figure 1a,b, were then processed and analyzed with MS to identify the constituent proteins. We also performed a semiquantitative assessment of the protein amounts by the method of spectral counting (SpC), which represents the total number of the MS/MS spectra for all peptides attributed to a matched protein. For each protein identified in the study by MS for the two samples, we calculated SpC in the two different experimental conditions: low plasma concentration (10%) and high plasma concentration (55%). The SpC of each protein identity was normalized to the protein mass and expressed as the relative protein quantity by applying the following equation:

$$\mathrm{NpSpC}_k = \left(\frac{(\mathrm{SpC}/M_w)_k}{\sum_{i=1}^{n} (\mathrm{SpC}/M_w)_i} \right) \times 100 \qquad (1)$$

where NpSpC_k is the percentage normalized spectral count for protein k, SpC is the spectral count identified, and M_w is the molecular weight in kDa for protein k. This correction takes into account the protein size and evaluates the real contribution of each protein to the hard corona composition.[4] Normalized SpC (NSpC) values for the most abundant proteins identified in the coronas of SiO_2 and $PSOSO_3$ NPs are given in Tables 3 and 4, and the full list is reported in Table S2 in the Supporting Information.

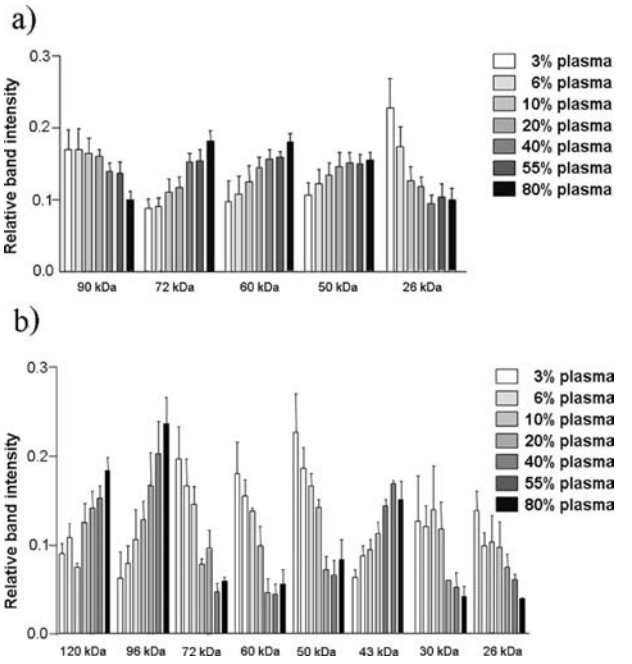

Figure 3. Relative amounts of the most abundant proteins adsorbed in the hard corona complexes of (a) 200 nm $PSOSO_3$ and (b) 200 nm SiO_2 NPs from plasma solutions at different concentrations (legend) after 1 h of incubation. The results are extracted as the relative intensity from the gels shown in Figure 1a,b, respectively. The error bars are expressed as the SD of the values obtained from five different gels (independent measurements). Table 3 reports the identities of the proteins determined by mass spectrometry analysis of selected bands cut from the gels reported in Figure 1a,b.

We have further calculated which proteins contribute most to the overall protein coronas, calculating the NSpC on proteins of different M_w ranges, and the outcome is presented in Figure 4. In principle, this analysis could be done exhaustively for all the bands, giving the nature and identity of all proteins that have been adsorbed to the different NPs. Here we wish only to illustrate the method and to identify those proteins most significantly exchanged following competitive binding as the plasma concentration is increased.

Despite the limitations due to particle aggregation, we use the study with 200 nm $PSOSO_3$ NPs to derive some qualitative insights (Figure 3a and Table 3): the 90 and 26 kDa proteins are prominent at the low plasma concentration, while the 70−50 kDa proteins dominate the hard corona composition at the higher plasma concentrations. However, from the MS results (Table 3), HSA (60 kDa) and fibrinogen (70−50 kDa depending on the chain) seem to be the main components of the hard corona for both samples (10% and 55%), together with immunoglobulin, which is known to have an affinity for hydrophobic regions,[27] and their amounts increase at higher plasma concentration (about 60% of the total protein hard corona from MS). Apolipoproteins and complement proteins (only the main hits are reported in Tables 3 and 4) are also enriched in the $PSOSO_3$ NPs corona, and their amount is decreased at higher protein concentration.[28,29] HSA and fibrinogen are both relatively abundant in plasma, and their prominence in the $PSOSO_3$ NPs corona is to be expected. Indeed, it is possible that the increasing amount of fibrinogen is connected to the formation of the particle clusters observed in the DCS results. Possibly immunoglobulin and complement proteins are the main components of

Table 3. Representative Hard Corona Proteins Associated with 200 nm $PSOSO_3$ NPs Incubated in 10% and 55% Plasma Solutions, As Identified by LC MS/MS[a]

			NSpC	
gel band M_w (kDa)	acc. no.[b]	protein identity	10% plasma	55% plasma
100	Q14624	inter-alpha-trypsin inhibitor heavy chain	1.84	2.80
90	P04196	histidine-rich glycoprotein	1.10	0.46
90	P02787	transferrin	1.43	0.42
90	P00747	plasminogen	1.32	0.59
90	P00751	complement factor B	0.57	0.22
90	P10643	complement component C7	0.24	0.13
72	P02671	fibrinogen alpha chain	5.74	16.19
72	P02768	serum albumin	5.28	4.15
72	P01042	kininogen-1	1.42	0.91
72	P04003	C4b-binding protein alpha chain	2.14	1.19
60	P02675	fibrinogen beta chain	12.69	25.19
60	P02774	vitamin D-binding protein	1.92	1.12
50	P02679	fibrinogen gamma chain	15.42	15.72
26	P02647	apolipoprotein A-I	2.86	5.58
12	P01834	Ig kappa chain C region	13.20	7.69

[a] Normalized spectral count (NSpC) values were calculated for each protein hit according to eq 1. The table contains only the most significant hits, while the full list of the most abundant proteins identified by MS is given in Table S2 in the Supporting Information. [b] Uniprot accession number.

Table 4. Representative Hard Corona Proteins Associated with 200 nm SiO_2 NPs Incubated in 10% and 55% Plasma Solutions, As Identified by LC MS/MS[a]

			NSpC	
gel band M_w (kDa)	acc. no.[b]	protein identity	10% plasma	55% plasma
500	P04114	apolipoprotein B 100	0.96	0.91
120	P07996	thrombospondin-1	0.01	1.37
90	P04196	histidine-rich glycoprotein	4.02	13.93
90	P00747	plasminogen	0.87	3.27
90	P02787	transferrin	0.02	0.52
72	P06396	gelsolin	–	0.63
90	P02671	fibrinogen alpha chain	15.43	4.88
72	P02768	serum albumin	1.80	9.67
72	P01042	kininogen-1	1.54	2.22
60	P02675	fibrinogen beta chain	23.92	7.99
50	P02679	fibrinogen gamma chain	18.40	6.52
50	P00748	coagulation factor XII	1.05	4.15
43	P49908	selenoprotein P	0.16	0.87
40	P02765	alpha-2-HS-glycoprotein	–	0.16
28	P02749	beta-2-glycoprotein	–	0.74
30	P02649	apolipoprotein E	3.13	3.87
30	P02746	complement C1q subcomponent beta	2.28	0.58
26	P02647	apolipoprotein A-I	9.45	14.83
12	P01834	Ig kappa chain C region	3.26	5.13

[a] Normalized spectral count (NSpC) values were calculated for each protein hit according to eq 1. This table contains only the most significant hits, while the full list of the most abundant proteins identified by MS is given in Table S1 in the Supporting Information. [b] Uniprot accession number.

the monomeric complexes, but the uncertainty here reflects the cautionary remarks about the methodology made above. We may compare with the results for 50 nm $PSOSO_3$ NPs (Figure 5), although here again the presence of aggregation implies the need for caution in interpretation. The general trend with increasing plasma concentration is preserved, independent of the size of the $PSOSO_3$ NPs, but the protein corona composition at the same plasma concentration is slightly different in the relative amount of each protein for the two different sized $PSOSO_3$ NPs, as can be seen by comparing the densitometry patterns reported in Figures 3a and 5b.

Interpreting the case of the 50 and 200 nm SiO_2 NP coronas is much simpler, since the dispersions are dominated by monomeric species whose coating thickness decreases with increasing protein

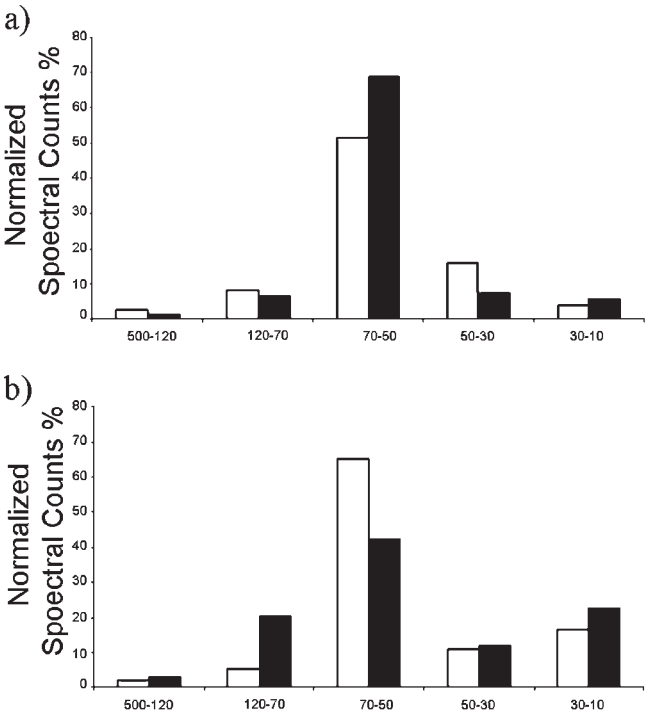

Figure 4. Normalized spectral counts (NSpC) of proteins of different M_w ranges contained in the hard corona from (a) 200 nm $PSOSO_3$ NPs and (b) 200 nm SiO_2 NPs, incubated for 1 h in 10% and 55% human plasma solutions.

concentration. Note that for the SiO_2 NP coronas, rapid changes in the intensity of most bands with variation of the corona composition occurs between 20% and 40% plasma concentration (Figure 3b), suggesting a co-operative phenomenon rather than independent competitive binding. MS results for the two representative 200 nm SiO_2 NP samples (at 10% and 55% plasma) suggest that the decrease in the intensity of the protein bands at 70−50 kDa with increasing plasma concentration is predominantly due to a decrease of the fibrinogen content, while proteins such as thrombospondin, histidine-rich glycoprotein, plasminogen, HSA, transferrin, selenoprotein, and α- and β-glycoprotein are enriched. It is quite remarkable to notice that at 55% plasma concentration, fibrinogen, which is one the most abundant proteins in the plasma (10−27 μmol/L), can be displaced by proteins whose concentration is significantly lower. A clear example is given by histidine-rich glycoprotein, whose concentration in human plasma is estimated to be around 1−3 μmol/L at 55% plasma; it becomes the major protein of the corona (∼19% NSpC), while the fibrinogen content is decreased by ∼10% NSpC (Table 4).[30,31] Immunoglobulin and complement proteins are also detected in the SiO_2 NP corona, and their amounts increase with increasing plasma concentration. The total apolipoprotein content (ApoE/ApoAI are most enriched and ApoB to a smaller extent) is significant (∼19% of NSpC) and increases with increasing plasma concentration. From the structural viewpoint, the main outcome is that at higher protein concentration, several of the larger plasma proteins are favored to adsorb onto the 200 nm SiO_2 NPs surface, with consequent displacement of fibrinogen and proteins in the 70−50 kDa range (Figure 3b). This is, at first sight, inconsistent with the overall decrease of the SiO_2 NP corona thickness with increasing plasma concentration as determined by DCS (Figure 3d). However, using the information on protein relative abundance and mass derived from MS NSpC

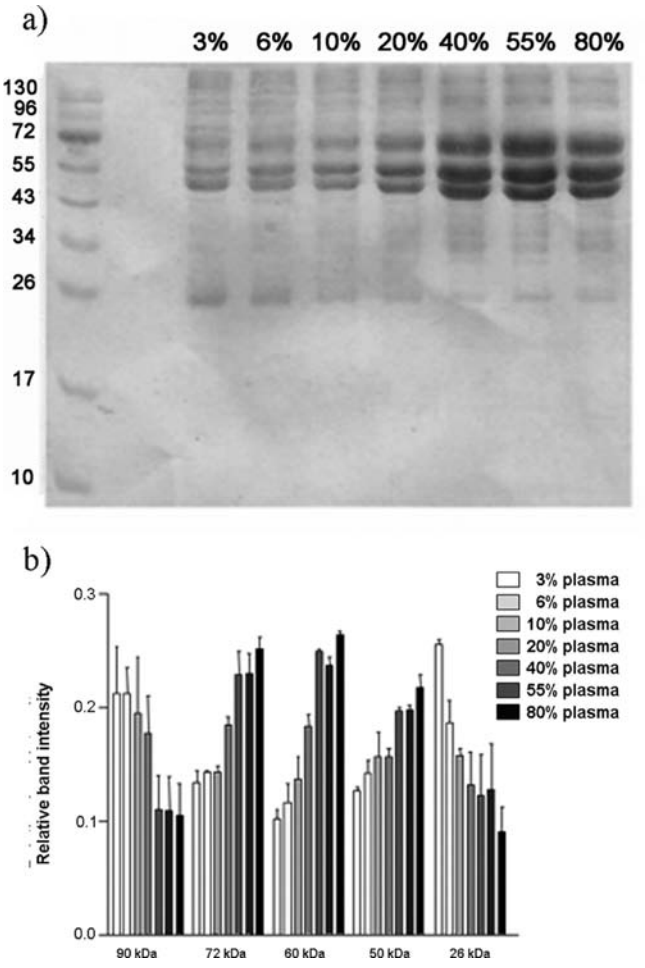

Figure 5. SDS−PAGE gel of human plasma proteins obtained from the hard corona of 50 nm $PSOSO_3$ NP−protein complexes free from excess plasma following incubation at different plasma concentrations. The molecular weights of the proteins in the standard ladder are reported on the left for reference. (b) Relative amounts of the most abundant proteins in the hard corona, calculated by densitometry, for proteins adsorbed on the surface of the 50 nm $PSOSO_3$ NPs. The error bars are expressed as the SD of the values obtained from three different gels.

analysis, we show that the major contribution to the protein corona thickness is from proteins in the 70−50 kDa range that are predominant in both $PSOSO_3$ and SiO_2 NP protein coronas (Figure 4).

It is worth briefly commenting on the situation for 50 nm SiO_2 NPs, although many of the conclusions are similar to those for the 200 nm SiO_2 NPs. As outlined above, for low protein-to-NP surface area ratios (surface more easily accessible to smaller proteins) there is some evidence of small amounts of particle aggregation from the DCS data (see Figure 6a,b). Also, in Table 5 we report DLS results of the same samples as measured with DCS. Together these results confirm the conclusion that the shift of the main particle peak to a higher nominal size than that of the bare NPs in PBS, observed for the lowest plasma concentration, is related to the formation of NP−protein clusters. The sample at the highest plasma concentration shows a shift of the peak toward a smaller NP−cluster size, corresponding to a protein shell of about 5 nm. DCS measurements *in situ* display the same trend, with the formation of larger particle−protein clusters at 6% plasma, which are dissociated at plasma concentration of 80% with the formation

dx.doi.org/10.1021/ja107583h |*J. Am. Chem. Soc.* 2011, 133, 2525–2534

of monomeric particle−protein complexes (Figure 6b). The small amount of particle aggregation of the 50 nm SiO_2 NPs at low plasma concentration might be due to incomplete surface coverage of the larger surface available for binding with respect to the analogous sample for bigger NPs. It certainly vanishes at higher plasma-to-particle surface ratios, restoring the situation described in some detail above. Again this suggests that the hard corona screens the primary surface, leading to a low zeta-potential, even for small additions of protein. An SDS−PAGE gel with the corresponding densitometry analysis for 50 nm SiO_2 NP−protein complexes is reported in Figure 6c,d, and the most striking difference between the 200 and 50 nm SiO_2 NPs occurs at low plasma concentrations, or at the largest surface area-to-protein ratios, which are not accessible for larger particles. There we see that several bands (for example 72, 60, and 50 kDa, related to fibrinogen) show an initial increase in relative intensity until 10% plasma concentration, followed by a progressive decrease with increasing plasma concentration, although the decrease is less steep than for the 200 nm SiO_2 NPs. Moreover, while the 120 kDa band increases with increasing plasma concentration for 200 nm SiO_2 NPs, it is unchanged within experimental error for the 50 nm SiO_2 NPs. It is possible that these differences reflect genuine differences in curvature at very low surface coverage. However, they may also reflect the small degree of aggregation present for SiO_2 NPs under these limiting conditions, possibly consistent with fibrinogen also playing a leading role. For higher surface-to-protein ratios one observes the same sort of competitive displacement as observed for the larger 200 nm SiO_2 particles.

We have also studied the composition of the hard corona of samples recovered after a 24 h period of incubation in the biological fluid for all plasma concentrations (see Figure S7 in the Supporting Information). The results of this study show quite different behavior for the two particles. For $PSOSO_3$ NPs, the protein corona composition does not change at different plasma concentrations after 24 h of incubation, as shown for the samples incubated for 1 h in plasma (Figure 3a). This result indicates that there is a time evolution of the corona, reaching the same protein composition at the longer incubation time for all plasma concentrations investigated. For SiO_2 NPs, by contrast, the relative intensity of the bands follows almost the same pattern with increasing plasma concentration as at shorter time of incubation, indicating that the protein corona does not evolve beyond 1 h and that the competitive binding process has reached equilibrium after 1 h of incubation.

In summary, for $PSOSO_3$ NPs, where the hydrophobic interaction is the driving force for protein adsorption with high entropic

Table 5. DLS and Zeta-Potential Data of 50 nm SiO_2 Particle−Corona Complexes Free from Excess Plasma, Obtained Following Incubation at Different Plasma Concentrations

% plasma	D_H[a] (nm)	PDI[b]	$\langle D_H \rangle$[c] (nm)	ζ-potential (mV)
0	75.9 ± 0.4	0.04	80.5 ± 0.4	−26.8 ± 0.1
6	182.2 ± 1.2	0.25	205.8 ± 1.3	−8.6 ± 0.2
80	128.5 ± 1.3	0.08	135.9 ± 1.5	−9.6 ± 0.2

[a] z-average hydrodynamic diameter extracted by cumulant analysis of the data. [b] Polydispersity index obtained from cumulant fitting. [c] Average hydrodynamic diameter determined from CONTIN size distribution.

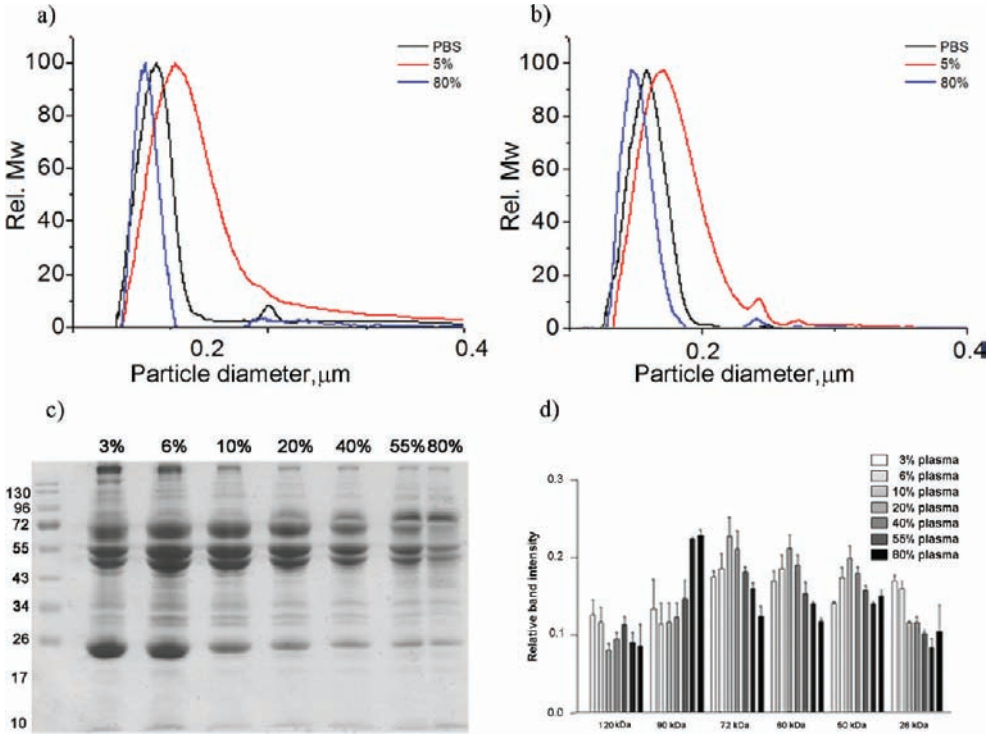

Figure 6. (a) DCS experiments of 50 nm SiO_2 particle−corona complexes free from excess plasma resuspended in PBS. The particle−corona complexes were isolated after 1 h of incubation in plasma solutions at different concentrations as shown in the legend. (b) DCS experiments of 50 nm SiO_2 particle−corona complexes "in situ" after incubation in plasma solutions at different concentrations. (c) SDS−PAGE gel of human plasma proteins obtained from 50 nm SiO_2 NP−protein complexes free from excess plasma following incubation at different plasma concentrations. The molecular weights of the proteins in the standard ladder are reported on the left for reference. (d) Relative amounts of the most abundant proteins in the hard corona, calculated by densitometry for proteins adsorbed on the surface of 50 nm SiO_2 NPs. The error bars are expressed as the SD of the values obtained from five different gels.

gain, due to both the release of the hydration shell from the NPs surface and possible changes expected in the conformation of the adsorbed proteins, proteins will also bind the NPs surface in electrostatically adverse conditions since the dehydration contribution will prevail over the repulsion. Protein adsorption onto $PSOSO_3$ NP surfaces certainly shields the negative surface potential. Partial protein unfolding, combined with any remaining uncovered NP surface, could then lead to formation of plasma−NP clusters. For negatively charged SiO_2 NPs, entropic gains on protein adsorption may be less, and the usual van der Waals interactions are supplemented by electrostatic and H-bonding effects. We also note in passing that the histidine-rich glycoprotein, whose total amount in the corona of SiO_2 NPs significantly increases with increasing plasma concentration, interacts with plasma proteins and may be carried into the corona by these effects.[32] Thus, the formation of the protein corona is more likely not a property of the isolated proteins alone but a collective, curvature-dependent phenomenon that leads to formation of a highly irreversible protein layer at the NPs surface. Attempts such as those above that assign the stability of the corona to individual particle surface−protein interactions must be interpreted with caution.

CONCLUSIONS

In this paper we have sought to initiate a framework for the disciplined physical−chemical study of the protein corona surrounding nanoparticles in a biological medium, while recognizing the reality that systems that are of biological interest are also often complex. In fact, it is now emerging clearly that besides size and shape, the other primary defining element of nanoscale objects in biological media is their long-lived ("hard") protein corona. Thus, we have combined studies on the composition of the protein corona at different plasma concentrations with structural data on the complexes both *in situ* and free from excess plasma. Where (as in these examples) the structure of the complexes *in situ* is almost identical to the structures after isolation from excess plasma, we may be relatively confident that the complexes we isolate are those also present *in situ*. This in turn enables a high degree of confidence in the meaning of the hard protein corona in a biological context.

The fact that the hard corona can quite significantly evolve (as in the case of SiO_2 NPs presented here) as one passes from a protein concentration appropriate to *in vitro* cell studies to the protein regime present during *in vivo* studies has deep implications for interpretation and extrapolation of experimental results. Turning to some more quantitative issues, in those cases where the system is relatively simple, one can really begin to frame a study of the adsorption isotherm (by analogy with a long tradition in physical chemistry) in which the NP surface coverage can be broken up into its constituent elements in a relatively complete manner. By applying methods of semiquantitative MS, we can even create the adsorption isotherms of the different components of the adsorbed layer and relate the amounts bound from MS to those found from structural studies.

Thus, it is a quite general observation that binding leads to relatively complete surface coverage for even low plasma concentrations. The protein concentration study also suggests a progressive displacement of proteins with lower affinity in favor of those with higher. However, there are significant differences compared to the more usual forms of adsorption, including the fact that, when formed, the protein layer is essentially irreversible on the time scales of the experiments carried out here. We interpret this to mean that the system seeks to lower its (initially high) surface energy by selecting and exchanging on shorter time scales from the whole set of proteins that diffuse to the surface. While the nature and formation of the NP−protein corona are at least developing some conceptual framework, with experimental methods growing capable of handling the challenge, the theoretical challenge of understanding why certain proteins are adsorbed in a competitive manner as described here is as yet unclear. Certainly there are many hints that this is a collective process, and therefore it will be difficult to rationalize on the basis of individual protein binding studies. Thus, while there is growing certainty that the corona is what is "seen" by the cell, there is as yet relatively little progress on why any NP chooses those particular proteins.

ASSOCIATED CONTENT

Supporting Information. Materials and sample preparation; detailed description of the core−shell method used to analyze the DCS data; and tables and figures showing simple physicochemical characterization of the NP dispersions in PBS, SDS−PAGE of 200 nm $PSOSO_3$ and SiO_2 NPs free from excess plasma at three different plasma concentrations, complete protein list and spectral count values of proteins identified by mass spectrometry analysis as being contained in the NP hard coronas, DCS data of $PSOSO_3$ NP−protein complexes *in situ* and free from excess plasma, SDS−PAGE and band densitometry of 200 nm $PSOSO_3$ and SiO_2 NP−protein complexes free from excess plasma following incubation with human plasma for 24 h, and SDS−PAGE and band densitometry of 50 nm $PSOSO_3$ and SiO_2 NP−protein complexes free from excess plasma following incubation with human plasma for 24 h. This material is available free of charge via the Internet at http://pubs.acs.org.

AUTHOR INFORMATION

Corresponding Author
francesca.baldelli@cbni.ucd.ie; kenneth.a.dawson@cbni.ucd.ie

ACKNOWLEDGMENT

This work was conducted under the framework of the INSPIRE programme, funded by the Irish Government's Programme for Research in Third Level Institutions, Cycle 4, National Development Plan 2007-2013. The SFI SRC BioNanoInteract (07 SRC B1155) also supported the research reported here. Additional financial support from FP6 IST project SIGHT (IST-2005-033700) and EU FP6 project NanoInteract (NMP4-CT-2006-033231) is acknowledged. Access to, and use of, instrumentation of the UCD Conway Mass Spectrometry Resource is gratefully acknowledged. The ESF Research Networking Programme EpitopeMap is also gratefully acknowledged.

REFERENCES

(1) Dobrovolskaia, M. A.; Patri, A. K.; Zheng, J.; Clogston, J. D.; Ayub, N.; Aggarwal, P.; Neun, B. W.; Hall, J. B.; McNeil, S. E. *Nanomedicine* **2009**, *5*, 106–117.

(2) Lundqvist, M.; Stigler, J.; Cedervall, T.; Elia, G.; Lynch, I.; Dawson, K. *Proc. Natl. Acad. Sci. U.S.A.* **2008**, *105*, 14265–14270.

(3) Cedervall, T.; Lynch, I.; Lindman, S.; Nilsson, H.; Thulin, E.; Linse, S.; Dawson, K. A. *Proc. Natl. Acad. Sci. U.S.A.* **2007**, *104*, 2050–2055.

(4) Walczyk, D.; Baldelli Bombelli, F.; Monopoli, M. P.; Lynch, I.; Dawson, K. *J. Am. Chem. Soc.* **2010**, *132*, 5761–5768.

(5) Lynch, I.; Salvati, A.; Dawson, K. A. *Nature Nanotechnol.* **2009**, *4*, 546–547.
(6) Lesniak, A.; Campbell, A.; Monopoli, M. P.; Lynch, I.; Salvati, A.; Dawson, K. A. *Biomaterials* **2010**, *31*, 9511–9518.
(7) Monopoli, M. P.; Baldelli Bombelli, F.; Dawson, K. A. *Nature Nanotechnol.* **2011**in press.
(8) Hellstrand, E.; Lynch, I.; Andersson, A.; Drakenberg, T.; Dahlback, B.; Dawson, K.; Linse, S.; Cedervall, T. *FEBS J.* **2009**, *276*, 3372–3381.
(9) Xin-Rui, X.; Monteiro-Riviere, N. A.; Riviere, J. E. *Nature Nanotechnol.* **2010**, *5*, 671–676.
(10) Roach, P.; Farrar, D.; Perry, C. C. *J. Am. Chem. Soc.* **2005**, *128*, 3939–3945.
(11) Shang, W.; Nuffer, J. H.; Muniz-Papandrea, V.; Colon, W.; Siegel, R. W.; Dordick, S. *Small* **2009**, *4*, 470–476.
(12) Cabaleiro-Lago, C.; Quinlan-Pluck, F.; Lynch, I.; Lindman, S.; Minogue, A. M.; Thulin, E.; Walsh, D. M.; Dawson, K. A.; Linse, S. *J. Am. Chem. Soc.* **2008**, *130*, 15437–15443.
(13) Linse, S.; Cabaleiro-Lago, C.; Xue, W. F.; Lynch, I.; Lindman, S.; Thulin, E.; Radford, S. E.; Dawson, K. A. *Proc. Natl. Acad. Sci. U.S.A.* **2007**, *104*, 8691–8696.
(14) Casals, E.; Pfaller, T.; Duschl, A.; Oostingh, G. J.; Puntes, V. *ACS Nano* **2010**, *4*, 3623–3632.
(15) Oberdörster, G. *J. Intern. Med.* **2010**, *267*, 89–105.
(16) Chithrani, B. D.; Chan, W. C. W. *Nano Lett.* **2007**, *7*, 1542.
(17) Ehrenberg, M. S.; Friedman, A. E.; Finkelstein, J. N.; Oberdorster, G.; McGrath, J. L. *Biomaterials* **2009**, *30*, 603–610.
(18) Dobrovolskaia, M. A.; Aggarwal, P.; Hall, J. B.; McNeil, S. E. *Mol. Pharmaceutics* **2008**, *5*, 487–495.
(19) Moghimi, S. M.; Hunter, A. C.; Murray, J. C. *Pharmacol. Rev.* **2001**, *53*, 283–318.
(20) Owens, D. E.; Peppas, N. A. *Int. J. Pharm.* **2006**, *307*, 215–222.
(21) Ishida, T.; Harashima, H.; Kiwada, H. *Curr. Drug Metab.* **2001**, *2*, 397–409.
(22) Camner, P.; Lundborg, M.; Lastbom, L.; Gerde, P.; Gross, N.; Jarstrand, C. *J. Appl. Physiol.* **2002**, *92*, 2608–2616.
(23) Ogawara, K.; Furumoto, K.; Nagayama, S.; Minato, K.; Higaki, K.; Kai, T.; Kimura, T. *J. Controlled Release* **2004**, *100*, 451–455.
(24) Kreuter, J. *J. Nanosci. Nanotechnol.* **2004**, *4*, 484–488.
(25) Kreuter, J.; Shamenkov, D.; Petrov, V.; Ramge, P.; Cychutek, K.; Koch-Brandt, C.; Alyautdin, R. *J. Drug Target* **2002**, *10*, 317–325.
(26) Jeon, S.; Lee, J.; Andrade, J.; De Gennes, P. *J. Colloid Interface Sci.* **1991**, *142*, 149–158.
(27) Zybailov, B.; Mosley, A. L.; Sardiu, M. E.; Coleman, M. K.; Florens, L.; Washburn, M. P. *J. Proteome Res.* **2006**, *5*, 2339–2347.
(28) van Oss, C. J.; Absolom, D. R.; Neuman, A. W. *Colloid Polym. Sci.* **1980**, *258*, 424–427.
(29) Chonn, A.; Cullis, P. R.; Devine, D. V. *J. Immunol.* **1991**, *146*, 4234–4241.
(30) Devine, D. V.; Wong, K.; Serrano, K.; Chonn, A.; Cullis, P. R. *Biochim. Biophys. Acta* **1994**, *1191*, 43–51.
(31) Hortin, G. L.; Sviridov, D.; Anderson, N. L. *Clin. Chem.* **2008**, *54*, 1608–1616.
(32) Borza, D.; Tatum, F.; Morgan, W. *Biochemistry* **1996**, *35*, 1925–1934.